Special Issue of the 8th International Advances in Applied Physics and Materials Science Congress (APMAS 2018)

NiTi SMA Parts Production with Different Porosity Ratios

S. Aksöz[a,*], Ü. Demir[b] and B. Bostan[c]

[a]Pamukkale University, Department of Metallurgical and Materials Engineering, Denizli, Turkey
[b]Incirli Vocational and Technical Anatolian High School, Ankara, Turkey
[c]Gazi University, Department of Metallurgical and Materials Engineering, Ankara, Turkey

NiTi SMA has widespread use in commercial and scientific fields with its recycling effect. Today, NiTi SMA alloys, which have different usage areas, are expected to have different properties. At the beginning of these properties, it is necessary to produce of the porosity structures (implant technology) and compact structure (high density material). For this reason, NiTi SMAs were produced with porous and compact structures in this study. Obtained theoretical densities were achieved from 57% to 90% in parts production.

DOI: 10.12693/APhysPolA.135.980

PACS/topics: NiTi SMAs, powders, porous structure

1. Introduction

The called of Nitinol shape memory alloys (SMA) has approximately the same chemical composition of Ni and Ti elements. These materials have unique shape memory properties, good damping effect, good wear properties and corrosion resistance. So, these alloys are widely used today. Also, these alloys have numerous uses in the industrial and medical applications [1, 2]. When the studies analyzed, Ni-Ti alloy produced by the SMA system, are usually produced via casting technique. However, properties such as; ductility, fracture resistance and superelasticity properties cannot be obtained satisfactorily in the samples produced by the melting method [3]. These properties can be directly affected by production conditions and environmental factors. The hydrogen in the NiTi parts structure are directly affected by the production parameters and environmental factors [4]. For this reason, new technology and application fields are needed in eliminating hydrogen content caused by environmental conditions. Powder metallurgy (PM) technique is at the forefront of these fields since it provides different production and shaping methods for NiTi alloys. Among the known PM methods; application areas such as metal injection molding (MIM), spark plasma sintering and hot izostatic pressing are among the leading of these methods [5–7]. The production method parameters are directly affect the transformation properties [8].

In this study; NiTi SMA pre-alloyed powders with a suitable binder system (binder content: PP + PEG8000 + SA) were mixed homogeneously and the raw parts were produced by hot pressing technique. Raw parts were debinded by using pure water first and then thermal debinding techniques. Finally, with using the different sintering temperatures application, the production of desired pore morphology was achieved.

2. Materials and method

NiTi powders were supplied as pre-alloyed from NANOVAL company. The powder size was about 10 μm. The shrinkage ratios and density measurements of the test specimens were calculated using TS EN 623-2 and TS 2305 standards. LEICA optical microscope (OM) and JEOL-JSM-6060LV Scanning Electron Microscope (SEM) were used to view the fractured surface. In order to standardize fractured surface analysis of manufactured parts, specimens were prepared according to the three-point bending standard (ASTM B312–96). The test was performed according to test apparatuses described in the standard (ASTM B528–05). Broken surface images were obtained on these samples.

In the production of the raw parts, first the binder and the powder were mixed to have a homogeneous mixture. Then the mixture was put in to the three-point bending mold that was at 180 °C. The mixture was held at this temperature for 15 min. Finally, it was pressed under 1 MPa pressure. The binder removal process was performed in two stages. In the first stage, pure water (for PEG 8000) was used. In the second stage thermal debinding process (at 200 °C, 400 °C, 600 °C for 60 min respectively and temperature increase rate was used 1 °C/min) was performed step by step. Samples were produced by sintering at 1000 °C, 1100 °C, 1150 °C, 1200 °C and 1250 °C for 60 min, respectively. Density of the produced parts were calculated by using the volume and the mass proportions of the porous structures [9]. In addition, density measurements were obtained by using the Archimedes method (depending on the weight values of the sintered pieces) while calculating the porosity ratios of the samples. In density calculations, the real density value was calculated according to the direct arc principle. The theoretical density and the percentage of porosity amounts were obtained according to mass and volume calculations and real density.

*corresponding author; e-mail: saksoz@pau.edu.tr

3. Results and discussion

The examination of fractured surface views of the samples is as shown in Fig. 1. Figure 1 shows the sample that was sintered at 1000 °C for 60 min. In Fig. 1a, three dimensional image of the sample was given. In Fig. 1b, the location of the fractured surface was shown. Figure 1c and d shows the OM and SEM images of the fractured surface.

In Fig. 2, the SEM images of the samples that were sintered at different temperatures were compared (1000 °C, 1100 °C, 1150 °C and 1200 °C). As the sintering temperature increased, it was determined that the bond between the powders also increased and the bond between the powders was strengthened by the temperature exceeding the liquid phase sintering temperature (Fig. 2c and d).

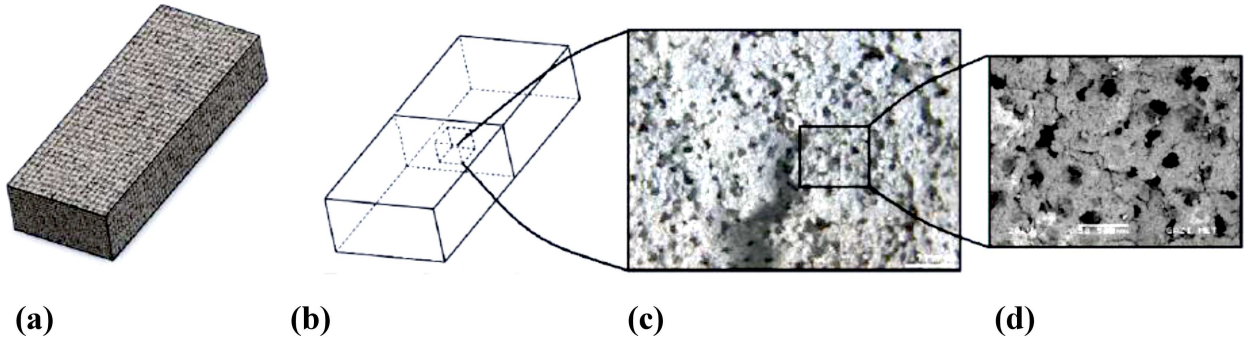

Fig. 1. Examination of the porosity structure of the produced NiTi particles, (a) three dimensional image, (b) the location of the fractured surface, the fractured surface (c) OM, and (d) SEM images.

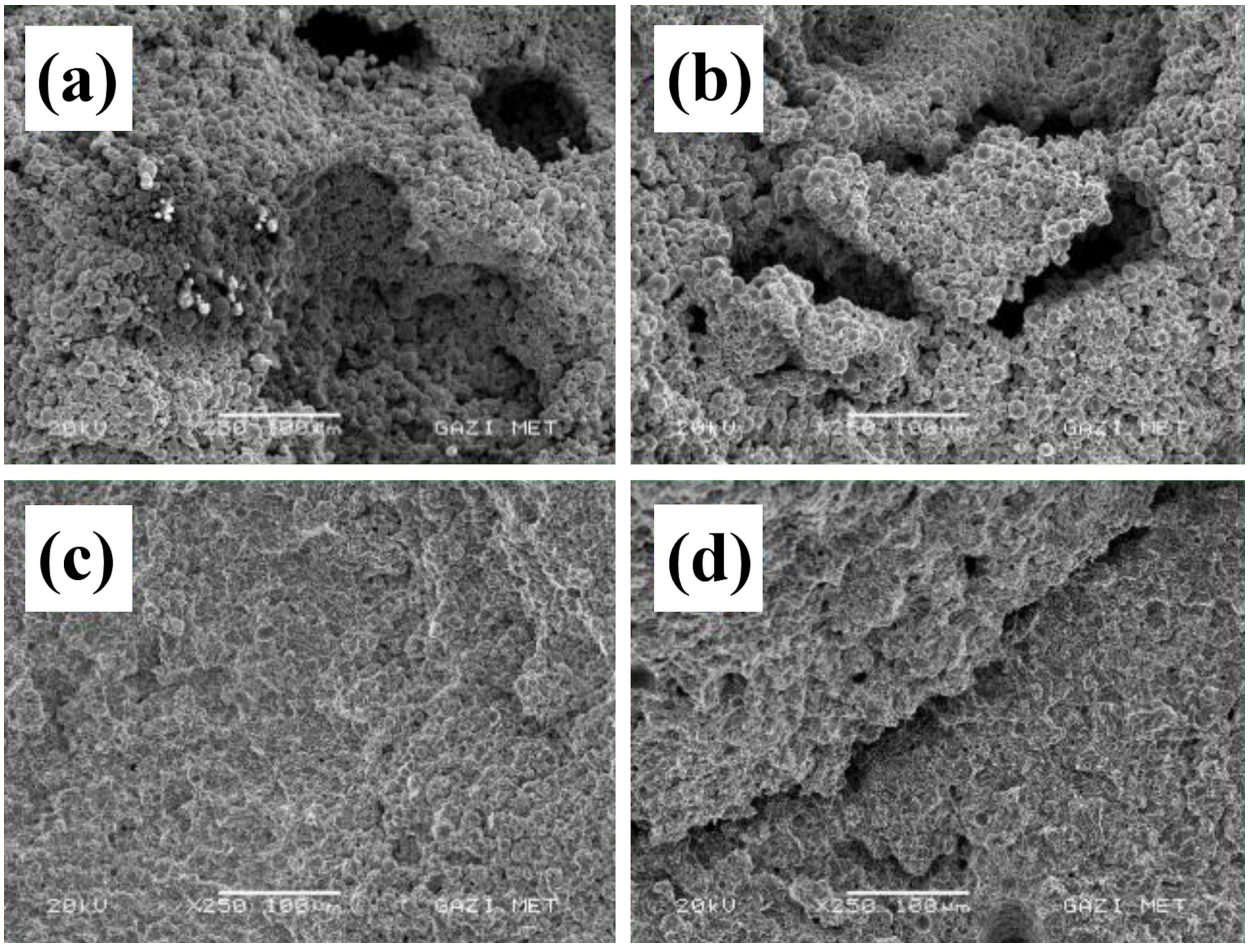

Fig. 2. Fractured parts SEM images of sintered for 60 min and at (a) 1000 °C, (b) 1100 °C, (c) 1150 °C and (d) 1200 °C, respectively.

With the sintering temperature reaching at 1200 °C, it ensured that the NiTi powders were now completely sintered and became a desired piece based on the sample formation (Fig. 2d). Choi et al. [10] studied the effect of different sintering temperatures on the microstructure and experimentally demonstrated that porosity decreased as the temperature increased in this work. When the pore morphology in Fig. 1d and Fig. 2a is examined, the homogeneous distribution of the pores within the structure shows that the binders move away homogenously from the structure during bonding removal and sintering processes. In Fig. 2b, it is seen that the pores started to close at 1100 °C, whereas in Fig. 2d the completely disappear of porosity when the temperature reach at 1200 °C is seen. Kaya et al. [11] reported that the porosity should be between 30% and 90% to obtain a good integration of the bone with NiTi alloys. Groot [12] reported that the most suitable pore size is in the range of 200–500 μm. Moreover, Itin et al. reported that the optimal pore sizes required for new bone growth should be within the range of 100–500 μm [13]. Tadic et al. [14] also reported that the pore sizes that should be found in the bone structure should be within the range of 50–500 μm. In the experimental studies, the size of porosities was in the range of 50 to 400 μm seen in the fractured surface images after sintering at 1000 °C and 1100 °C for 60 min. So, it was shown that the size and the morphology of the porosity shown in the literature could be produced by the methodology described in this paper. Thus, the method used was suitable for tissue structure (Fig. 2a and b).

It is known that the density increases with increasing sintering temperature [15]. Figure 3 shows the real density data depending on the temperature. While the real density value at 1000 °C was 3.818 g/cm^3, the density value reaches up to 5.98 g/cm^3 at 1250 °C. Figure 4 shows the theoretical density and porosity ratios depending on the temperature. At a sintering temperature of 1250 °C the theoretical density reaches up to 90%

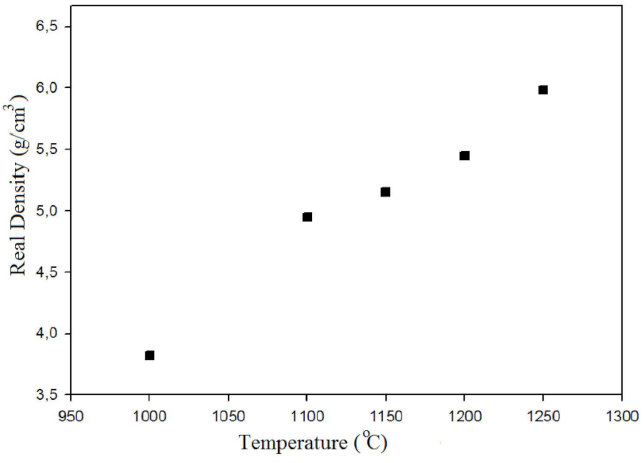

Fig. 3. Real densities of samples sintered for 60 min at different sintering temperature.

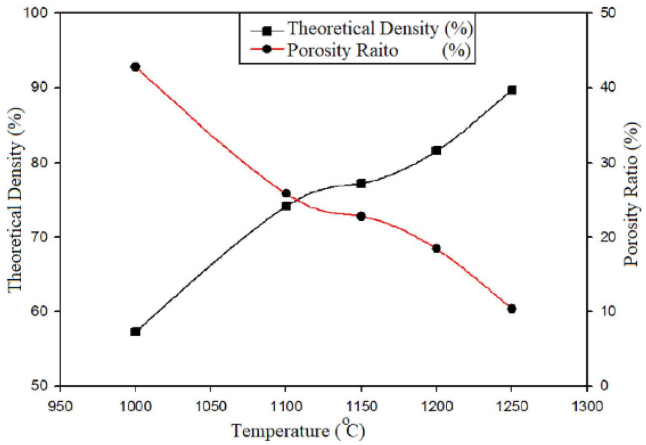

Fig. 4. Porosity and theoretical density ratios of sintered parts, for 60 min at 1000 °C, 1100 °C, 1150 °C, 1200 °C, and 1250 °C, respectively.

of the real density, the porosity is about 10%. The Kryachek study [16] reported that density increased with increasing sintering temperature and Levenfeld [15] found that porosity decreased due to increased density. Similar to the literature, density also increased with increasing sintering temperature and porosity ratio was also decreased in this experimental work as shown in Fig. 2a–d and Fig. 4.

The size and quantity of pores are directly related to sintering temperature and the size of the powder. Figure 5 shows the effect of sintering temperature on the volumetric shrinkage ratio. At the sintering temperature of 1000 °C the shrinkage is about 3%, when the temperature reaches 1250 °C, the shrinkage achieves 28%. In similar studies, Wu and his colleagues [17] achieved the success in producing porous specimens for implant materials by producing NiTi alloys with 42% porosity using hot isostatic pressing. With the methods described in this paper, materials could be produced with about

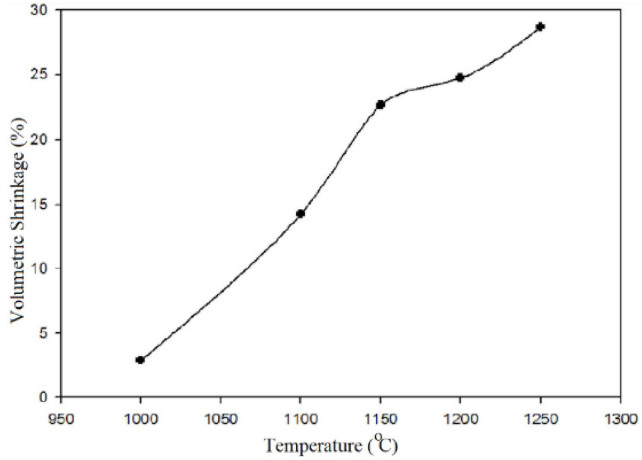

Fig. 5. Parts volumetric shrinkages values of sintered for 60 min and at 1000 °C, 1100 °C, 1150 °C, 1200 °C, and 1250 °C, respectively.

43% of real density at a sintering temperature of 1000 °C (Fig. 4). The suitability of the debinding and sintering parameters study could be also seen from the absence of faults and smooth micro-surfaces of the sintered parts (Fig. 2).

4. Conclusion

The analyze of the results in this study leads to the following conclusions:

1. The method described in this paper could be used for tissue structures based on the Tadic works,
2. By altering the sintering temperatures, different porosity ratios, density, volumetric shrinkages could be obtained. This material could be applied to many areas such as; biomaterials, space and aviation materials, transportation,
3. This methodology is an alternative method to conventional casting process,
4. The suitability of the debinding and sintering parameters for the study can be seen with the absence of faults in the view of sintered parts and achieved of smooth micro-surfaces,
5. It is known with previous studies; the pore sizes must be found in bone structure should be within the range of 50–500 μm. In this study, the production of approximately the same pore sizes by sintering at 1000-1100 °C can be used as material suitable for tissue structure,
6. Depending on the sintering temperature, there were homogenously distributed pores both on the surfaces and inside of the parts.

Acknowledgments

This study was financially supported by Pamukkale University, Scientific Research Projects Unit (PAU BAP ADEP) under the project number of 2018KRM002-351.

References

[1] S. Aksöz, B. Bostan, *J. Polytechnic*, **21**, 437 (2018).
[2] A. Ota, Y. Yazaki, K. Yokoyama, J. Sakai, *Mater. Trans.* **50**, 1843 (2009).
[3] M.H. Elahinia, M. Hashemi, M. Tabesh, S.B. Bhaduri, *Prog. Mater. Sci.* **57**, 911 (2012).
[4] T. Ogawa, K. Yokoyama, K. Asaoka, J. Sakai, *Mater. Sci. Eng. A* **393**, 239 (2005).
[5] S. Aksöz, *Arab. J. Sci. Eng.* **42**, 2573 (2017).
[6] S. Aksöz, B. Bostan, in: *International Multidisciplinary Microscopy Congress*, Springer Proceedings in Physics, Springer Switzerland, 2014, p. 129.
[7] C. Shearwood, Y.Q. Fu, L. Yu, K.A. Khor, *Scripta Mater.* **52**, 455 (2006).
[8] S. Aksöz, G. Altınışık, E.E. Elverişli, B. Bostan, *Gazi Univ. J. Sci. C* **6**, 570 (2018).
[9] T. Goryczka, J.V. Humbeeck, *J. Achiev. Mater. Manufact. Engin.* **17**, 1 (2006).
[10] J.-P. Choi, G.-Y. Lee, J.-I. Song, W.-S. Lee, J.-S. Lee, *Powder Technol.* **279**, 196 (2015).
[11] M. Kaya, N. Orhan, G. Tosun, *Mater. Sci. Technol.* **26**, 522 (2010).
[12] K. de Groot, *Biomater.* **1**, 47 (1980).
[13] V.I. Itin, V.E. Gjunter, S.A. Shabalovskaya, R.L.C. Sacheva, *Mater. Character.* **32**, 179 (1994).
[14] D. Tadic, F. Beckmann, T. Donath, M. Epple, *Materiwiss Werkst* **35**, 240 (2004).
[15] B. Levenfeld, A. Gruzza, A. Varez, J.M. Toralba, *Powder Met.* **43**, 233 (2000).
[16] V. M. Kryachek, *Powder Metall. Metal Ceram.* **43**, 336 (2004).
[17] S.L. Wu, P.K. Chu, X.M. Liu, C.Y. Chung, J.P.Y. Ho, C.L. Chu, S.C. Tjong, K.W.K. Yeung, W.W. Lu, K.M.C. Cheung, K.D.K Luk, *J. Biomed. Mat. Res. A*, **79**, 139 (2006).